arXiv:nucl-th/0307105v2 12 Nov 2003

Determining the Θ^+ quantum numbers through the $K^+p \to \pi^+K^+n$ reaction

T. Hyodo[a]*, A. Hosaka[a] and E. Oset[b]

February 8, 2008

[a] *Research Center for Nuclear Physics (RCNP), Ibaraki, Osaka 567-0047, Japan*

[b] *Departmento de Física Teórica and IFIC, Centro Mixto Universidad de Valencia-CSIC, Institutos de Investigación de Paterna, Aptd. 22085, 46071 Valencia, Spain*

Abstract

We study the $K^+p \to \pi^+K^+n$ reaction with some kinematics suited to the production of the Θ^+ resonance recently observed. We show that, independently of the quantum numbers of the Θ^+, a resonance signal is always observed in the K^+ forward direction. In addition, we also show how a combined consideration of the strength at

*E-mail : hyodo@rcnp.osaka-u.ac.jp

the peak, and the angular dependence of polarization observables can help determine the Θ^+ quantum numbers using the present reaction.

PACS: 13.75.-n, 12.39.Fe

Keywords: Θ^+ baryon, Spin parity determination

A recent experiment by LEPS collaboration at SPring-8/Osaka [1] has found a clear signal for an $S = +1$ positive charge resonance around 1540 MeV. The finding, also confirmed by DIANA at ITEP [2], CLAS at Jefferson Lab. [3] and SAPHIR at ELSA [4], might correspond to the exotic state predicted by Diakonov *et al.* in Ref. [5].

Since the mass appears almost precisely at the value of the theoretical prediction of Ref. [5] using the chiral quark soliton model, the observed state may be identified with the Θ-baryon [1] ($(I, J^P) = (0, 1/2^+)$) of five quarks ($uudd\bar{s}$), although spin, parity and isospin are not yet determined experimentally. Theoretically, the parity of Θ^+ is interesting and important. In the naive quark model, all quarks can be put in the lowest $1/2^+$ orbit. Since $\bar{s}$ carries negative parity, the $\Theta(uudd\bar{s})$ in this naive picture would have negative parity, in contrast with the prediction of the chiral quark soliton model [5]. There are several theoretical studies for this resonance [6, 7, 8, 9, 10] and recently lattice simulation has been also carried out [11].

The experiment at SPring-8 was performed with the reaction $\gamma n \to K^- K^+ n$ with the $K^+ n$ mass distribution showing the peak of the resonance

[1] In Ref. [5], this state was denoted as Z^+. However, as a standard notation of baryon resonances, Θ^+ has been recently proposed by Diakonov.

(Θ^+). The target neutron was in a ^{12}C nucleus, but a test was carefully carried out in order to select neutrons from the Fermi sea with small longitudinal momentum which accurately gave the invariant mass of the K^+n system by evaluating $(p_\gamma + p_n - p_{K^-})$ with the assumption that the initial neutron is at rest. The test is convincing by selecting the final K^+ events moving predominantly in the forward direction. However, a dispersion of the invariant mass of around 10 MeV from the Fermi motion is unavoidable. In the experiment at Jefferson Lab, the reaction $\gamma d \to K^+K^-pn$ was performed. The measurement of the charged final particles determines completely the kinematics and allows one to reconstruct the K^+n invariant mass where the Θ^+ is seen. Yet, elimination of the K^+K^- resonant peak of the ϕ and the $\Lambda(1520)$ for K^-p events is needed to extract the signal. Also the dynamical mechanisms of photo-induced reactions in this energy region are generally very complicated.

In such a situation, alternative reactions based on known elementary processes are most welcome in order to increase our knowledge of the resonance and help determine properties like spin, isospin and parity. Some hadron-induced and photon-induced reactions are studied theoretically in Refs. [12, 13, 14]. We present one particularly suited reaction with the process

$$K^+p \to \pi^+K^+n \ . \tag{1}$$

Characteristic features of this reaction are:

1. The K^+n invariant mass can be precisely determined by measuring the

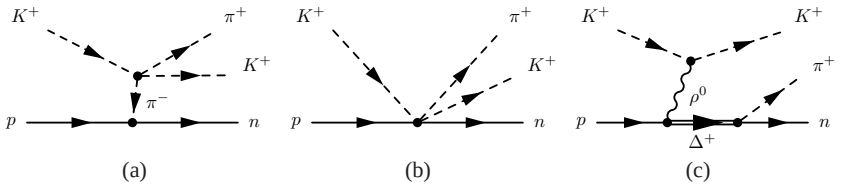

Figure 1: Feynman diagrams of the reaction $K^+p \to \pi^+K^+n$ in the model of Ref. [15].

π^+ momentum alone.

2. It is expected that the initial state of the reaction is rather simple, since we do not know of a K^+p resonance that could complicate the initial system.

3. By choosing small momenta of the π^+, we shall be also far away from the Δ^+ resonance and hence the $K^+n(\Theta^+)$ resonance signal can be more clearly seen.

A successful model for the reaction (1) was considered in Ref. [15], consisting of the mechanisms depicted in terms of Feynman diagrams in Fig. 1. The term (a) (pion pole) and (b) (contact term), which are easily obtained from the chiral Lagrangians involving meson-meson [16, 17] and meson-baryon interaction [18, 19, 20] are spin flip terms (proportional to $\boldsymbol{\sigma}$), while the ρ exchange term (diagram (c)) contains both a spin flip and a non spin flip part. Having an amplitude proportional to $\boldsymbol{\sigma}$ is important in the present context in order to have a test of the parity of the resonance. Hence we choose a situation, with the final pion momentum $\boldsymbol{p}_{\pi^+}$ small compared to

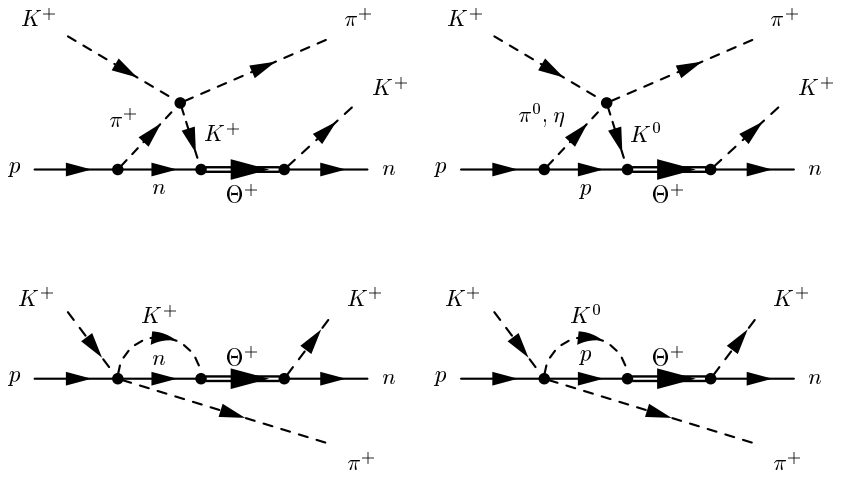

Figure 2: Feynman diagrams of the reaction $K^+p \to \pi^+K^+n$ with the Θ^+ resonance.

the momentum of the initial kaon, such that the diagram (c), which contains the $\boldsymbol{S} \cdot \boldsymbol{p}_{\pi^+}$ operator can be safely neglected. The terms of Fig. 1 (a) and (b) will provide the bulk for this reaction. If there is a resonant state for K^+n then this will be seen in the final state interaction of this system. This means that in addition to the diagrams (a) and (b) of Fig. 1, we shall have those in Fig. 2. If the resonance is an s-wave K^+n resonance then $J^P = 1/2^-$. If it is a p-wave resonance, we can have $J^P = 1/2^+, 3/2^+$. We shall study all these three possibilities, but couplings of higher partial waves are not considered here.

The restriction to have small pion momenta eliminates also other possible resonant contributions like the one in the diagram of Fig. 3, which involves the $\boldsymbol{\sigma} \cdot \boldsymbol{p}_{\pi^+}$ coupling. One could in principle have negative parity resonances instead of the intermediate neutron, which involve an s-wave πNN^* coupling,

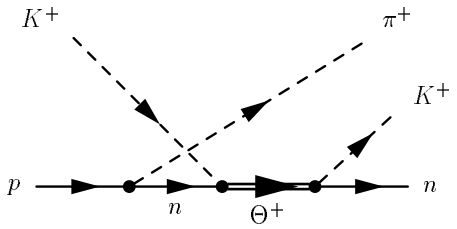

Figure 3: Feynman diagrams of the reaction $K^+p \to \pi^+K^+n$ with the Θ^+ resonance.

but the lightest one would be the $N^*(1535)$ which would be very much off shell, rendering the contribution of the diagram negligible. Note also that the consideration of N^* resonances instead of the intermediate n, p states in Fig 2 is not usually done in chiral dynamics calculations since it is accounted for by means of counterterms, or subtraction constants in the loop function which can be equally taken into account by the choice of the cut off [21].

The resonance contribution to the $K^+n(K^0p) \to K^+n$ amplitudes are given by

$$\begin{aligned} t^{(s)}_{K^+n(K^0p)\to K^+n} &= \frac{(\pm)g^2_{K^+n}}{M_I - M_R + i\Gamma/2} \ , \\ t^{(p,1/2)}_{K^+n(K^0p)\to K^+n} &= \frac{(\pm)\bar{g}^2_{K^+n}(\boldsymbol{\sigma}\cdot\boldsymbol{q}')(\boldsymbol{\sigma}\cdot\boldsymbol{q})}{M_I - M_R + i\Gamma/2} \ , \\ t^{(p,3/2)}_{K^+n(K^0p)\to K^+n} &= \frac{(\pm)\tilde{g}^2_{K^+n}(\boldsymbol{S}\cdot\boldsymbol{q}')(\boldsymbol{S}^\dagger\cdot\boldsymbol{q})}{M_I - M_R + i\Gamma/2} \ , \end{aligned} \tag{2}$$

for s-wave and p-wave with $J^P = 1/2^+, 3/2^+$, where M_I is the energy of the K^+n system in the center of mass frame, M_R and Γ the mass and width of the resonance $(1540\,\text{MeV}, 20\,\text{MeV})$, and q and q' the momenta of the initial and final kaon, respectively. $\boldsymbol{S}^\dagger$ is the spin transition operator from spin 1/2

to 3/2 states. The signs + and − stand for the $K^0 p \to K^+ n$ amplitude in the case one has $I = 1$ or $I = 0$ for the Θ^+ resonance. We are implicitly assuming isospin conservation and hence we do not consider the possibility of $I = 2$, suggested in Ref. [6], which implies isospin violation in its decay to KN. The values of g, $\bar{g}$ and $\tilde{g}$ can be obtained from the Θ^+ width

$$g^2_{K^+n} = \frac{\pi M_R \Gamma}{Mq} \ , \quad \bar{g}^2_{K^+n} = \frac{\pi M_R \Gamma}{Mq^3} \ , \quad \tilde{g}^2_{K^+n} = \frac{3\pi M_R \Gamma}{Mq^3} \ . \tag{3}$$

A straightforward evaluation of the meson pole and contact terms (see also Ref. [22]) leads to the $K^+ n \to \pi^+ KN$ amplitudes

$$-it_i = (a_i + b_i \boldsymbol{k}_{in} \cdot \boldsymbol{q}' + c_i)\boldsymbol{\sigma} \cdot \boldsymbol{k}_{in} + (-a_i - b_i \boldsymbol{k}_{in} \cdot \boldsymbol{q}' + d_i)\boldsymbol{\sigma} \cdot \boldsymbol{q}' \ , \tag{4}$$

where $i = 1, 2$ stands for the final state $K^+ n, K^0 p$ respectively and k_{in} and q' are the initial and final K^+ momenta. The coefficients a_i and b_i are from meson exchange terms, and c_i and d_i from contact terms. They are given by

$$\begin{aligned} a_1 =& -\frac{1}{3f^2}(m_K^2 - 2m_\pi \omega(q) - \omega(k_{in})\omega(q) - \omega(k_{in})m_\pi) \\ & \cdot \frac{\sqrt{2}(D+F)}{2f} \frac{1}{p_{ex}^2 - m_\pi^2} \ , \end{aligned} \tag{5}$$

$$a_2 = a_{2,\pi} + a_{2,\eta} \ , \tag{6}$$

$$a_{2,\pi} = -\frac{1}{\sqrt{2}f^2} m_\pi (\omega(k_{in}) + \omega(q)) \cdot \frac{D+F}{2f} \frac{1}{p_{ex}^2 - m_\pi^2} \ , \tag{7}$$

$$\begin{aligned} a_{2,\eta} =& \frac{1}{\sqrt{6}f^2}(2\omega(k_{in})\omega(q) + m_\pi \omega(q) - m_\pi \omega(k_{in}) - \frac{2}{3}m_K^2 + \frac{2}{3}m_\pi^2) \\ & \cdot \frac{3F - D}{2\sqrt{3}f} \frac{1}{p_{ex}^2 - m_\eta^2} \ , \end{aligned} \tag{8}$$

$$b_1 = -\frac{1}{3f^2} \cdot \frac{\sqrt{2}(D+F)}{2f} \frac{1}{p_{ex}^2 - m_\pi^2} \ , \tag{9}$$

$$b_2 = b_{2,\pi} + b_{2,\eta} \ , \tag{10}$$

$$b_{2,\pi} = 0 \ , \tag{11}$$

$$b_{2,\eta} = -\frac{1}{\sqrt{6}f^2} \cdot \frac{3F-D}{\sqrt{3}f} \frac{1}{p_{ex}^2 - m_\eta^2} \ , \tag{12}$$

$$c_1 = \frac{\sqrt{2}(D+F)}{12f^3} \ , \tag{13}$$

$$c_2 = -\frac{\sqrt{2}D}{12f^3} \ , \tag{14}$$

$$d_1 = \frac{\sqrt{2}(D+F)}{24f^3} \ , \tag{15}$$

$$d_2 = -\frac{D+3F}{2} \frac{\sqrt{2}}{12f^3} \ , \tag{16}$$

where p_{ex} is the momentum of the meson exchanged in the meson pole term. The three momentum of the final pion is already neglected in these formulae.

Now let us turn to the resonance diagrams of Fig. 2 containing a loop integral, which is initiated by the tree diagrams of Figs. 1 (a) and (b). The momentum of K^+ is now an internal variable $\boldsymbol{q}$. In performing the loop integral, the fact that $\boldsymbol{k}_{in}$ is reasonably larger than $\boldsymbol{q}$, allows us to make an angle average of the meson propagator which simplifies the integrals. Furthermore, as shown in Ref. [23] and also found in the meson baryon scattering processes [24], the amplitude $K^+p \to \pi^+K^+n$ factorizes inside the loops with its on-shell value, which means in Eqs. (5)-(16) one takes

$$\omega(q) = \frac{M_I^2 + m_K^2 - M_N^2}{2M_I}$$

Note that since we have chosen the π^+ momentum small, the K^+n final state is also approximately in its center of mass frame and we assume this kinematics in the variables.

When taking into account KN scattering through the Θ^+ resonance, as depicted in Fig. 2, the $K^+p \to \pi^+K^+n$ amplitude is given by

$$-i\tilde{t} = -it_1 - i\tilde{t}_1 - i\tilde{t}_2 \tag{17}$$

where $\tilde{t}_1$ and $\tilde{t}_2$ account for the scattering terms with intermediate K^+n and K^0p, respectively. They are given by

$$\begin{aligned}
-i\tilde{t}_i^{(s)} =& \frac{g^2_{K^+n}}{M_I - M_R + i\Gamma/2}\left\{G(M_I)(a_i + c_i) - \frac{1}{3}\bar{G}(M_I)b_i\right\}\boldsymbol{\sigma}\cdot\boldsymbol{k}_{in}S_I(i)\ , \\
-i\tilde{t}_i^{(p,1/2)} =& \frac{\bar{g}^2_{K^+n}}{M_I - M_R + i\Gamma/2}\bar{G}(M_I)\left\{\frac{1}{3}b_i\boldsymbol{k}^2_{in} - a_i + d_i\right\}\boldsymbol{\sigma}\cdot\boldsymbol{q}'S_I(i)\ , \\
-i\tilde{t}_i^{(p,3/2)} =& \frac{\tilde{g}^2_{K^+n}}{M_I - M_R + i\Gamma/2}\bar{G}(M_I)\frac{1}{3}b_i\left\{(\boldsymbol{k}_{in}\cdot\boldsymbol{q}')(\boldsymbol{\sigma}\cdot\boldsymbol{k}_{in}) - \frac{1}{3}\boldsymbol{k}^2_{in}\boldsymbol{\sigma}\cdot\boldsymbol{q}'\right\}S_I(i)\ ,
\end{aligned} \tag{18}$$

for s- and p-wave, and $i = 1, 2$ for K^+n and K^0p respectively. $S_I(i)$ gives the sign for the K^+n and K^0p components in $I = 0$ and 1. Thus $S_0(1) = 1$, $S_1(1) = 1$, $S_0(2) = -1$ and $S_1(2) = 1$. The function $G(M_I)$ is the loop function of a meson and a baryon propagator

$$G(M_I) = \int \frac{d^3q}{(2\pi)^3}\frac{1}{2\omega(q)}\frac{M}{E(q)}\frac{1}{M_I - \omega(q) - E(q) + i\epsilon}\ , \tag{19}$$

regularized in Ref. [24] with a three momentum cut off $q_{max} = 630$ MeV/c to reproduce the data of $\bar{K}N$ scattering. We use here the same function. Similarly, $\bar{G}(M_I)$ is the same integral but with a factor $\boldsymbol{q}^2$ in the numerator of Eq. (19).

For completeness, we include a recoil factor in all terms to account for $\mathcal{O}(p/M)$ relativistic corrections for the $\gamma^\mu\gamma_5\partial_\mu$ BBM vertex, which is given

by

$$F_i = \left(1 - \frac{p_{ex}^{0(i)}}{2M_p}\right) \ . \tag{20}$$

In addition, we also consider the strong form factor of the MMB vertex for which we take a standard monopole and static form factor

$$F_f(\boldsymbol{p}) = \frac{\Lambda^2 - m_\pi^2}{\Lambda^2 + \boldsymbol{p}^2} \tag{21}$$

with $\Lambda \sim 900$ MeV. This form factor is applied both to the meson pole and contact terms to preserve the subtle cancellation of off shell terms shown in Ref. [23]. Inside the loops, for the reasons exposed above, the product of the form factor and propagator is replaced by its angle averaged expression which simplifies the formulae. This is implicit in the a_i, b_i coefficients of Eqs. (18).

We take an initial three momenta of K^+ in the Laboratory frame $k_{in}(Lab) = 850$ MeV/c ($\sqrt{s} = 1722$ MeV), which allows us to span K^+n invariant masses up to $M_I = 1580$ MeV, thus covering the peak of the Θ^+, and still is small enough to have negligible π^+ momenta with respect to the one of the incoming K^+. The double differential cross section is given by ($\cos\theta$ is the angle between $\boldsymbol{k}_{in}$ and $\boldsymbol{q}'$

$$\begin{aligned}\frac{d^2\sigma}{dM_I d\cos\theta} =& \frac{1}{(2\pi)^3}\frac{1}{8s}\frac{M^2}{\lambda^{1/2}(s, M^2, m_K^2)}\frac{1}{M_I} \\ & \times \bar{\Sigma}\Sigma|t|^2\lambda^{1/2}(s, M_I^2, m_\pi^2)\lambda^{1/2}(M_I^2, M^2, m_K^2) \ .\end{aligned} \tag{22}$$

where $\lambda(x, y, z)$ is the Källen function defined by $\lambda(x, y, z) = x^2 + y^2 + z^2 - 2xy - 2yz - 2zx$. We show below the results for the different options of isospin, spin and parity of the Θ^+.

In Fig. 4, we show the invariant mass distribution $d^2\sigma/dM_I d\cos\theta$ in the K^+ forward direction ($\theta = 0$). Here we see that, independently of the quantum numbers of Θ^+, a resonance signal is always observed. The signals for the resonance are quite clear for the case of $I, J^P = 0, 1/2^+$ (these would be the quantum numbers predicted in Ref. [5]) and $I, J^P = 0, 1/2^-$, while in the other cases the signal is weaker and the background more important, particularly for the case of $I, J^P = 0, 1/2^+$. With estimated uncertainties in the theory of the order of 20-30 percent, from the approximations done, the strength of the peak at the resonance could already serve to discriminate among the several possibilities.

We have used a Θ^+ width of 20 MeV, but experimentally it could be smaller since the experimental widths observed are mostly coming from the experimental resolution [25, 26]. It is easy to see how this would change our results. By looking at Eqs. (18) at the peak of the resonance distribution and considering the couplings obtained in Eq. (3) we see that the strength at the peak is independent of Γ. Only the width of the calculated distributions would be smaller for smaller Γ.

The angular dependence is shown in Fig. 5 for a value of $M_I = 1540$ MeV. What we observe there is that the angular dependence is rather weak in all cases. The background has a weak angular dependence and the resonance signal for this unpolarized cross section has only angular dependence for the case of spin 3/2, where it goes as $(3\cos^2\theta + 1)$, but in this case the resonance contribution is much smaller than the background and this angular dependence is not very visible. The different inflexions of the cross section

at $\theta = 0$ are probably too small to be discriminated in an experiment, hence the conclusion is that this unpolarized observable does not shed any further light on the quantum numbers.

Let us now see what can one learn with resorting to polarization measurements. Eqs. (18) account for the resonance contribution to the process. The interesting finding there is that if the Θ^+ couples to K^+n in s-wave (hence negative parity) the amplitude goes as $\boldsymbol{\sigma} \cdot \boldsymbol{k}_{in}$ while if it couples in p-wave it has a term $\boldsymbol{\sigma} \cdot \boldsymbol{q}'$. Hence, a possible polarization test to determine which one of the couplings the resonance chooses is to measure the cross section for initial proton polarization $1/2$ in the direction z ($\boldsymbol{k}_{in}$) and final neutron polarization $-1/2$ (the experiment can be equally done with K^0p in the final state, which makes the nucleon detection easier). In this spin flip amplitude $\langle -1/2|t| + 1/2\rangle$, the $\boldsymbol{\sigma} \cdot \boldsymbol{k}_{in}$ term vanishes. With this test the resonance signal disappears for the s-wave case, while the $\boldsymbol{\sigma} \cdot \boldsymbol{q}'$ operator of the p-wave case would have a finite matrix element proportional to $q' \sin\theta$. This means, away from the forward direction of the final kaon, the appearance of a resonant peak in the cross section would indicate a p-wave coupling and hence a positive parity resonance.

In Fig. 6 we show the results for the polarized cross section measured at 90 degrees as a function of the invariant mass. The two cases with s-wave do not show any resonant shape since only the background contributes. All the other cross sections are quite reduced to the point that the only sizeable resonant peak comes from the $I, J^P = 0, 1/2^+$ case. A clear experimental signal of the resonance in this observable would unequivocally indicate the

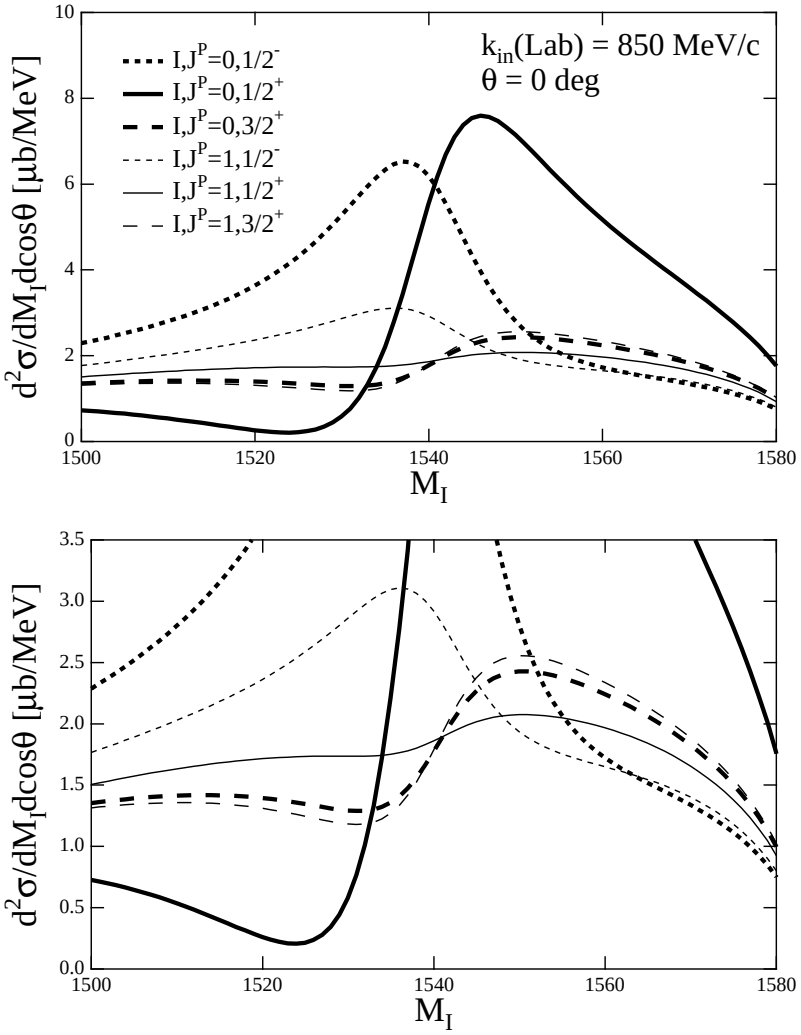

Figure 4: The double differential cross sections $d^2\sigma/dM_I d\cos\theta$ with $\theta = 0$ (forward direction) for $I = 0, 1$ and $J^P = 1/2^-, 1/2^+, 3/2^+$. Below, detail of the lower part of the upper figure of the panel.

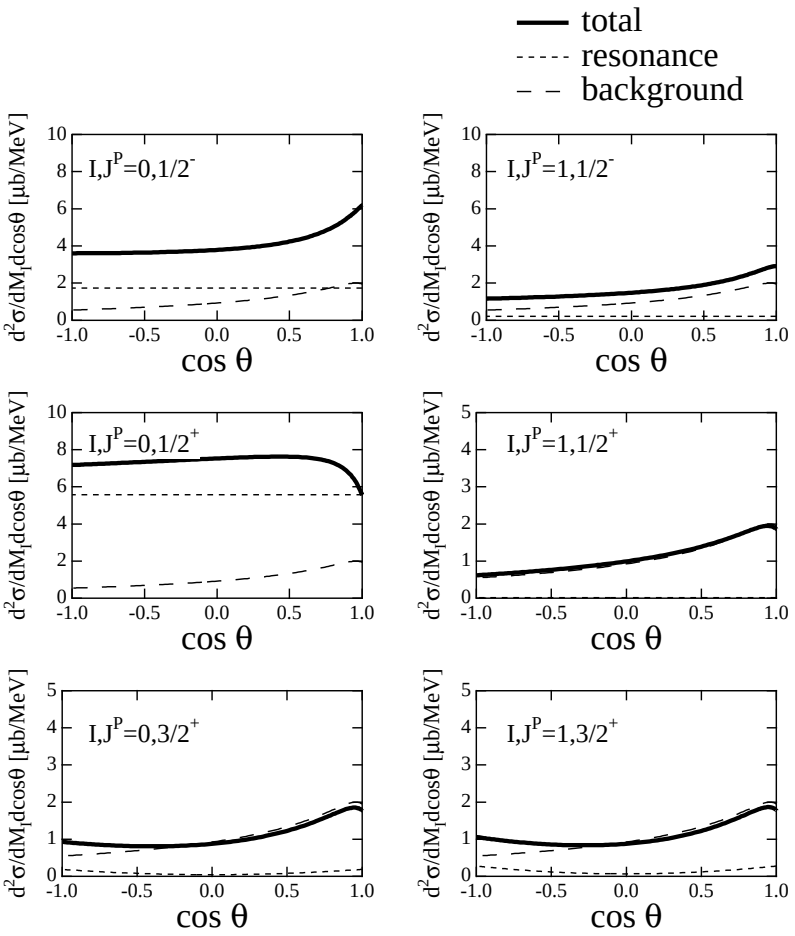

Figure 5: Angular dependence of the double differential cross sections $d^2\sigma/dM_I d\cos\theta$ with $M_I = 1540$ MeV at the resonance peak for $I = 0, 1$ and $J^P = 1/2^-, 1/2^+, 3/2^+$.

quantum numbers as $I, J^P = 0, 1/2^+$.

Finally, in Fig. 7 we show the angular dependence of the polarized cross section for a fixed value of the invariant mass of 1540 MeV. The angular distributions look all of them similar, as a consequence of the weakness or disappearance of the resonance contribution, with a peak around 35 degrees, except for the case of $I, J^P = 0, 1/2^+$, where the peak is found around 80 degrees and has a much larger size than in the other cases.

Since 100 % polarization can not be achieved in actual experiments, we have computed cross sections for the case of incomplete polarization. We have then found that for a typical polarization rate of about 80 % [2], the previous results shown in Figs. 6 and 7 do not change much. For instance, as shown in Fig. 8, the cross section decreases about 10 % for $I, J^P = 0, 1/2^+$. For $I, J^P = 0, 1/2^-$, the peak value at around $M_I \sim 1540$ MeV increases, since there is no resonance contribution for the case of 100 % polarization. However, the absolute value is small as compared to the one of $J^P = 1/2^+$. For the totally unpolarized case, the $1/2^+$ cross section reduces to about half of the polarized one, while the $1/2^-$ cross section shows a sizable peak. The tendency for other cross sections such as angular dependence is also similar.

In summary, we have shown here an elementary reaction, $K^+p \to \pi^+K^+n$, where, based on the present knowledge of the Θ^+ resonance, we can make predictions for Θ^+ production cross sections. We see that, independently of the Θ^+ quantum numbers, a resonance signal is always seen in the forward direction of the final K^+. The strength at the peak could serve to

[2]We define the polarization rate by $(N_+ - N_-)/(N_+ + N_-)$.

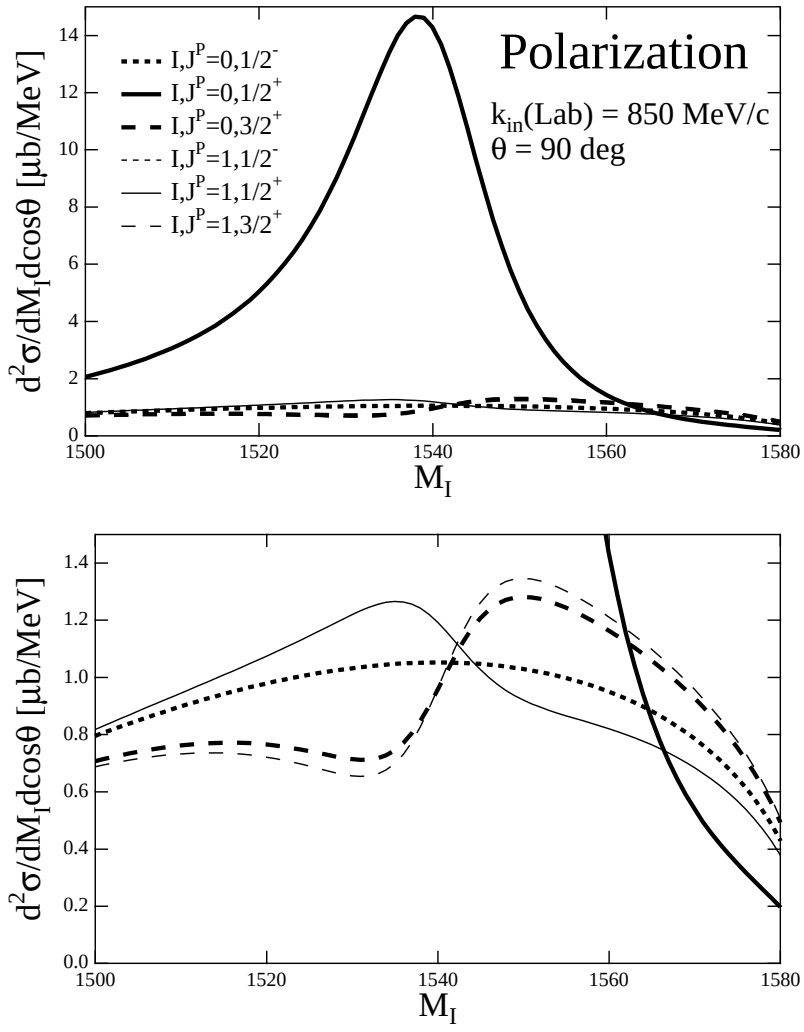

Figure 6: The double differential cross sections $d^2\sigma/dM_I d\cos\theta$ with $\theta = 0$ (forward direction) for $I = 0, 1$ and $J^P = 1/2^-, 1/2^+, 3/2^+$. Below, detail of the lower part of the upper figure of the panel. In these figures, thick and thin short-dashed lines ($J^P = 1/2^-$) coincide, since there is only background contribution. In the upper panel, the almost identical results of $J^P = 3/2^+$ drawn by the two long-dashed lines also coincide.

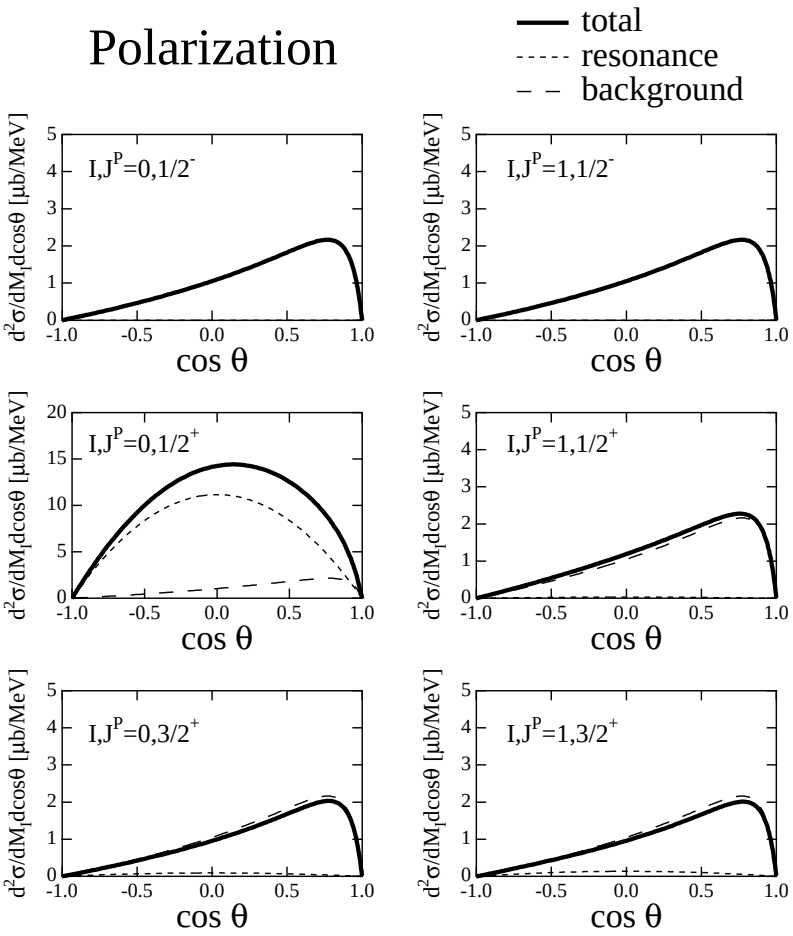

Figure 7: Angular dependence of the double differential cross sections of polarized amplitude with $M_I = 1540$ MeV at the resonance peak for $I = 0, 1$ and $J^P = 1/2^-, 1/2^+, 3/2^+$.

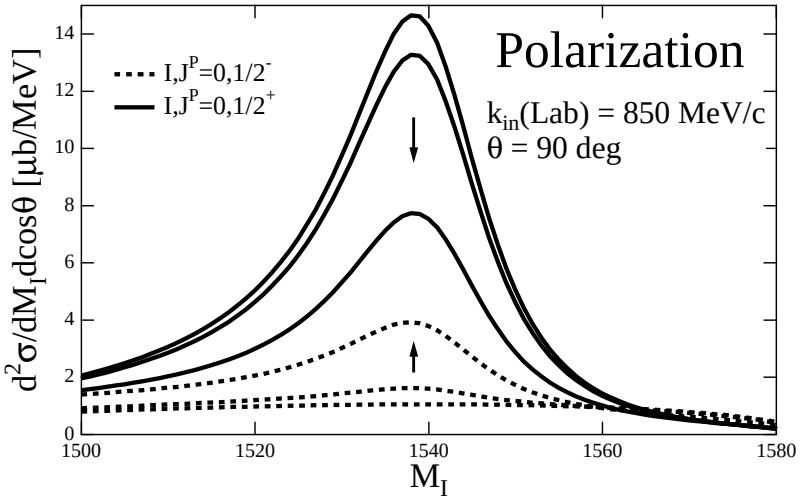

Figure 8: Effects of incomplete polarization on the double differential cross sections at $\theta = 90$ degrees. Three solid and dashed lines are for 100 %, 80 % and 0 % (along the direction of an arrow) polarization for $J^P = 1/2^{\pm}$ and $I = 0$.

discriminate among several cases. Further measurements of a polarized cross section could serve to further eliminate other possibilities. In particular, a strong signal seen at 90 degrees for the polarized cross section would clearly indicate that the quantum numbers of the resonance are those predicted in Ref. [5].

The reaction suggested here can be easily performed and, in particular, a small change in the set up of the experiment at ITEP used to detect the Θ^+ could be made to perform the reaction. The determination of the quantum numbers of the Θ^+ is an essential step to further investigate its nature. The implementation of the present reaction would represent a step forward in this direction.

Acknowledgments

This work is supported by the Japan-Europe (Spain) Research Cooperation Program of Japan Society for the Promotion of Science (JSPS) and Spanish Council for Scientific Research (CSIC), which enabled E. O. to visit RCNP, Osaka and T. H. and A. H. to visit IFIC, Valencia. This work is also supported in part by DGICYT projects BFM2000-1326, and the EU network EURIDICE contract HPRN-CT-2002-00311.

References

[1] LEPS, T. Nakano et al., Phys. Rev. Lett. 91 (2003) 012002.

[2] DIANA, V.V. Barmin et al., hep-ex/0304040.

[3] CLAS, S. Stepanyan, hep-ex/0307018.

[4] SAPHIR, J. Barth et al., hep-ex/0307083.

[5] D. Diakonov, V. Petrov and M.V. Polyakov, Z. Phys. A359 (1997) 305.

[6] S. Capstick, P. R. Page and W. Roberts, Phys. Lett. B **570** (2003) 185.

[7] F. Stancu and D. O. Riska, hep-ph/0307010.

[8] M. Karliner and H. J. Lipkin, hep-ph/0307243.

[9] A. Hosaka, Phys. Lett. B **571** (2003) 55.

[10] R. L. Jaffe and F. Wilczek, hep-ph/0307341.

[11] F. Csikor, Z. Fodor, S. D. Katz and T. G. Kovacs, hep-lat/0309090.

[12] W. Liu and C. M. Ko, nucl-th/0308034.

[13] S. I. Nam, A. Hosaka and H. -Ch. Kim, hep-ph/0308313.

[14] W. Liu and C. M. Ko, nucl-th/0309023.

[15] E. Oset and M.J. Vicente Vacas, Phys. Lett. B386 (1996) 39.

[16] J. Gasser and H. Leutwyler, Nucl. Phys. B250 (1985) 465.

[17] U.G. Meissner, Rept. Prog. Phys. 56 (1993) 903.

[18] A. Pich, Rept. Prog. Phys. 58 (1995) 563.

[19] G. Ecker, Prog. Part. Nucl. Phys. 35 (1995) 1.

[20] V. Bernard, N. Kaiser and U.G. Meissner, Int. J. Mod. Phys. E4 (1995) 193.

[21] J. A. Oller and U. G. Meissner, Phys. Lett. B **500** (2001) 263.

[22] U.G. Meissner, E. Oset and A. Pich, Phys. Lett. B353 (1995) 161.

[23] T. Hyodo, A. Hosaka, E. Oset, A. Ramos, and M. J. V. Vacas, nucl-th/0307005.

[24] E. Oset and A. Ramos, Nucl. Phys. A635 (1998) 99.

[25] S. Nussinov, hep-ph/0307357.

[26] R. A. Arndt, I. I. Strakovsky and R. L. Workman, nucl-th/0308012.